





Cytotoxicity and apoptotic gene expression in an in vitro model of the blood–brain barrier following exposure to poly(butylcyanoacrylate) nanoparticles

Andrew M. Hall, Ruth Hemmer, Robert Spaulding, Hanna N. Wetzel, Joseph Curcio, Bernhard A. Sabel, Petra Henrich-Noack, Sarah Pixley, Tracy Hopkins, Richard L. Boyce, Patrick J. Schultheis & Kristi L. Haik


To cite this article: Andrew M. Hall, Ruth Hemmer, Robert Spaulding, Hanna N. Wetzel, Joseph Curcio, Bernhard A. Sabel, Petra Henrich-Noack, Sarah Pixley, Tracy Hopkins, Richard L. Boyce, Patrick J. Schultheis & Kristi L. Haik (2016) Cytotoxicity and apoptotic gene expression in an in vitro model of the blood–brain barrier following exposure to poly(butylcyanoacrylate) nanoparticles, *Journal of Drug Targeting*, 24:7, 635–644, DOI: [10.3109/1061186X.2015.1132222](https://doi.org/10.3109/1061186X.2015.1132222)

To link to this article: <http://dx.doi.org/10.3109/1061186X.2015.1132222>

 View supplementary material [↗](#)

 Accepted author version posted online: 27 Dec 2015.
Published online: 05 Feb 2016.

 Submit your article to this journal [↗](#)

 Article views: 69

 View related articles [↗](#)

 View Crossmark data [↗](#)

ORIGINAL ARTICLE

Cytotoxicity and apoptotic gene expression in an *in vitro* model of the blood–brain barrier following exposure to poly(butylcyanoacrylate) nanoparticles

Andrew M. Hall^{a,b}, Ruth Hemmer^a, Robert Spaulding^a, Hanna N. Wetzel^a, Joseph Curcio^a, Bernhard A. Sabel^c, Petra Henrich-Noack^c, Sarah Pixley^d, Tracy Hopkins^d, Richard L. Boyce^a, Patrick J. Schultheis^a and Kristi L. Haik^a

^aDepartment of Biological Sciences, Northern Kentucky University, Highland Heights, KY, USA; ^bDepartment of Chemistry, Northern Kentucky University, Highland Heights, KY, USA; ^cInstitute of Medical Psychology, Otto-von-Guericke University, Magdeburg, Germany; ^dMolecular and Cellular Physiology Department, University of Cincinnati Medical Center, Cincinnati, OH, USA

ABSTRACT

Background Poly(butylcyanoacrylate) (PBCA) nanoparticles (NPs) loaded with doxorubicin (DOX) and coated with polysorbate 80 (PS80) have shown efficacy in the treatment of rat glioblastoma. However, cytotoxicity of this treatment remains unclear.

Purpose The purpose of this study was to investigate cytotoxicity and apoptotic gene expression using a proven *in vitro* co-culture model of the blood–brain barrier.

Methods The co-cultures were exposed to uncoated PBCA NPs, PBCA-PS80 NPs or PBCA-PS80-DOX NPs at varying concentrations and evaluated using a resazurin-based cytotoxicity assay and an 84-gene apoptosis RT-PCR array.

Results The cytotoxicity assays showed PBCA-PS80-DOX NPs exhibited a decrease in metabolic function at lower concentrations than uncoated PBCA NPs and PBCA-PS80 NPs. The apoptosis arrays showed differential expression of 18 genes in PBCA-PS80-DOX treated cells compared to the untreated control.

Discussion As expected, the cytotoxicity assays demonstrated enhanced dose-dependent toxicity in the DOX loaded NPs. The differentially expressed apoptotic genes participate in both the tumor necrosis factor receptor-1 and mitochondria-associated apoptotic pathways implicated in current DOX chemotherapeutic toxicity.

Conclusion The following data suggest that the cytotoxic effect may be attributed to DOX and not the NPs themselves, further supporting the use of PBCA-PS80 NPs as an effective drug delivery vehicle for treating central nervous system conditions.

ARTICLE HISTORY

Received 25 August 2015
Revised 23 October 2015
Accepted 3 December 2015
Published online 3 February 2016

KEYWORDS

Apoptosis; blood–brain barrier; doxorubicin; poly(butylcyanoacrylate) nanoparticles; polysorbate 80

Background

Over 1.5 billion people worldwide suffer from central nervous system (CNS) diseases, disorders and injuries.[1] Many of these neurological conditions lack satisfactory treatments, creating a need for improved drug therapies. Drug delivery to the brain presents a considerable challenge due to the highly selective permeability of the blood–brain barrier (BBB). This selectivity is necessary for the BBB to maintain cerebral homeostasis and prevent foreign molecules from gaining access to the brain. The BBB is primarily composed of brain capillary endothelial cells (BCECs) and is anatomically and physiologically supported by multiple structures, including: pericytes, astrocytes, microglial cells and neurons.[2,3] Integral membrane proteins between BCECs form tight junctions which, along with multidrug resistance proteins (like P-glycoprotein), are largely responsible for the high selectivity currently reported to block more than 98% of CNS drugs.[4,5] Consequently, it is essential to develop new methods for safe and effective drug delivery to the CNS.

Nanotechnology provides an approach to deliver drugs to targets within the CNS while also enhancing the drugs' efficacy. Nanoparticle (NP)-drug complexes have the potential to transport drugs across the BBB to a target using a non-invasive, systemic delivery method.[6] A wide range of CNS drugs can be delivered

to the brain via NPs without modifying the drug molecule itself. These include small drugs, peptides and proteins and may cross the BBB using a variety of mechanisms that are not fully elucidated.[3,7–10] Despite a lack of concrete mechanistic understanding, a number of promising brain-specific NP delivery systems have been developed and evaluated.[2,11–17] Many studies showing effective drug transport across the BBB use low molecular weight poly(butylcyanoacrylate) (PBCA) NPs.[18] The addition of a polysorbate 80 (Tween[®] 80, PS80) coating facilitated delivery and increased the efficacy of otherwise non-diffusible drugs, including the chemotherapeutic agent doxorubicin (DOX).[19–22] When DOX was bound to PBCA NPs, coated with PS80 and administered to rats intravenously, the drug was detected in the brain at therapeutic concentrations. Increased efficacy of the DOX-loaded, PS80-coated PBCA NPs drug delivery system was validated in a rat model of intracranial glioblastoma when a significant anti-tumor effect was observed following intravenous tail vein injection.[23]

The proposed mechanisms of action for DOX suggest it binds to multiple molecular targets, including DNA-associated enzymes that intercalate DNA base pairs, topoisomerases I and II and proteins responsible for activation of the tumor suppressor p53. This broad range of targets allows the drug to play a role in both tumor anti-proliferation and cytotoxicity, often through apoptotic

mechanisms.[24–28] This same diversity in molecular targets can often lead to unintended toxicity to non-tumorous tissues throughout the body. DOX is capable of inducing apoptosis, necrosis (especially at high doses), and possibly autophagy in healthy tissue in the brain, liver, kidney and heart.[24,29,30] Systemic administration of DOX causes an increase in reactive oxygen species (ROS) that is recognized by toll-like receptor 4, which subsequently increases the level of the inflammatory cytokine tumor necrosis factor-alpha (Tnf), the ligand for the tumor necrosis factor receptor-1 (Tnfr1). Both ROS-mediated mitochondrial permeability and Tnfr1 activation are known to induce apoptosis in many cells.[31,32] The ability of DOX to impede neoplastic cells and slow disease progression is limited by its unintended toxicity on noncancerous cells in the human body. It is therefore essential to devise a drug delivery system that would reduce or eliminate the adverse effects of DOX. This may be accomplished by reducing the total dose and selectively targeting greater concentrations of the drug to the tumor.

Although a great deal of evidence supports the therapeutic potential of PBCA NPs, there are concerns that NPs themselves might be toxic.[33] The same properties that influence NP uptake by cells, such as surface charge and hydrophobicity, may also contribute to unintended toxicity.[23,34–36] Specifically, Gelperina and colleagues showed that properties of the coating surfactant and other formulation parameters, such as core polymer, drug attachment and surface functional groups may be responsible for brain delivery of nanoparticles.[37] These same characteristics have also been shown to affect NP toxicity.[38,39] It is imperative to understand the toxicity of NPs used in the CNS, as they may compromise the integrity of the BBB and cause acute or long-term consequences.

The objective of this study was evaluate cytotoxicity and differential gene expression of PBCA NPs with and without the addition of DOX in model of the BBB using a co-culture of primary rat brain astrocytes and BCECs. Hyperspectral imaging techniques were also used to identify the presence of PBCA-PS80-Rhodamine within astrocytes, indicating the ability of this NP complex to cross the astrocyte cell membrane. *In vitro* resazurin-based toxicology assays were used to analyze cytotoxicity due to mitochondrial events and an 84-gene PCR array was used to monitor differential apoptotic gene expression.

Methods

Ethics statement

All animals were treated in accordance with the National Institutes of Health PHS Policy on Humane Care and Use of Laboratory Animals (2002), and all animal protocols were reviewed and approved by the Northern Kentucky University Institutional Animal Care and Use Committee.

Nanoparticle preparation

Uncoated PBCA NPs (102 nm) and PBCA-PS80 NPs (130 nm) were obtained from The Institute of Medical Psychology (Otto-von-Guericke University, Magdeburg, Germany). For the uncoated PBCA NPs, two separate solutions were prepared: Solution A (0.024 g sodium dodecyl sulfate [SDS] and 4.8 ml 0.1 M phosphoric acid) and Solution B (0.077 g soy bean oil and 1.2 g butylcyanoacrylate [at 4 °C]). Solution B was then mixed with Solution A, and a mini-emulsion was produced with an ultrasonic homogenizer (71% of maximum output; 4 min). In parallel, a beaker with 4.8 ml of 0.1 M ammonia solution was put on a magnetic stirrer. The milky

mini-emulsion was slowly poured into the ammonia solution and the pH was adjusted to 7 within the next 5 min by adding ammonia solution. The resulting suspension was stored in the dark at 6 °C.

For the PBCA-PS80 NPs, two separate solutions were prepared: Solution A (0.513 g Polysorbate 80 and 9 ml 0.8 M phosphoric acid) and Solution B (0.09 g soy bean oil and 2.3 g butylcyanoacrylate [at 4 °C]). Solution B was then mixed with Solution A. The mixture was placed in an ice bath, and a mini-emulsion was produced with an ultrasonic homogenizer (70% of maximum output; 2 min). In parallel, a beaker with 9 ml of 0.8 M ammonia solution was put on a magnetic stirrer. The milky mini-emulsion was slowly poured into the ammonia solution and the pH was adjusted to 7 within the next few minutes by adding ammonia solution. The resulting suspension was stored in the dark at 6 °C. The NPs containing DOX (160 nm) and the rhodamine-123 labeled NPs (160 nm) were purchased from Capsulation Nanoscience AG (Berlin, Germany).

Cell isolation and co-culture

Astrocytes and BCECs were isolated from rat brain cortex and co-cultured utilizing procedures adapted from Garcia-Garcia et al. and Szabo et al. [40,41]. For BCEC isolation, brain cortex from two-week old Sprague-Dawley rats (Harlan Laboratories, Indianapolis, IN) was isolated, mechanically disrupted, and incubated at 37 °C in DMEM/F12 (Invitrogen, Pittsburgh, PA) containing 0.1 mg/ml collagenase-dispase (Sigma-Aldrich, St. Louis, MO), 30 µg/ml gentamycin (Sigma-Aldrich) and 0.25 µg/ml amphotericin B (Sigma-Aldrich) for 1.5 h. Cold DMEM/F12 was added and the homogenate was centrifuged and the pellet was re-suspended in 25% bovine serum albumin (Sigma-Aldrich) and centrifuged again. This pellet was then digested for 1 h at 37 °C in DMEM/F12/collagenase-dispase/gentamycin/amphotericin B solution as above. This digest was then filtered through nylon mesh with a 10 µm filter (Millipore, Darmstadt, Germany) and washed three times with DMEM/F12. Capillary fragments were recovered and seeded onto a 75 cm² tissue culture flask coated with collagen type IV (Sigma-Aldrich) in EBMTM-2 culture medium (Lonza, Basel, Switzerland) with 10% FBS (Atlanta Biologicals, Flowery Branch, GA), 3 µg/ml puromycin (Sigma-Aldrich), 30 µg/ml gentamycin, and 0.25 µg/ml amphotericin B and then incubated at 5% CO₂ and 37 °C. After 3 days, the media was changed to EBMTM-2 culture medium supplemented with EGMTM-2 MV Singlequots[®] (Lonza). Initial treatment of the capillaries with puromycin eliminates contaminating cells, because puromycin is toxic to cells lacking P-gp, which is expressed at a high level in rat BCECs. This treatment allows rat BCECs to proliferate with the appropriate shape and transendothelial electrical resistance.[40,41]

For astrocyte isolation, 1–3 days old Sprague-Dawley rat brains were extracted, the meninges were removed, and the cortex was isolated. The cortex was then disaggregated with 10 ml of 7.5 mM EDTA (Sigma-Aldrich) in Ca²⁺/Mg²⁺-free PBS using a 10 ml pipette for 10 min at room temperature. The homogenized tissue was passed through an 80 µm filter (Millipore), and the cells were washed off the filter into a 75 cm² tissue culture flask with 15 ml of DMEM/F12 containing 20% FBS and an antibiotic solution of 10 000 units/ml of penicillin, 10 000 µg/ml of streptomycin, and 25 µg/ml of Fungizone[®] (Invitrogen). Cells were incubated at 5% CO₂ and 37 °C, and the medium was changed every 3 days. After 7 days, the flasks were shaken for 24 h at 37 °C to eliminate the contaminating microglia. Immunocytochemistry was performed to verify cellular morphology of both astrocytes and BCECs (Supplemental Figure S1).

Co-culture was accomplished as follows: after the first or second passage, astrocytes were grown to approximately 90% confluency and plated on Falcon® 24-well (cytotoxicity assays) or 96-well plates (RT-PCR) (Thermo Fisher Scientific) at 150 000 cells/well and 30 000 cells/well respectively. The following day, BCECs (first or second passage; at approximately 90% confluency) were plated at the same concentrations on top of the astrocytes. The cells were incubated at 5% CO₂ and 37 °C for 6–7 days with regular media changes using 50% astrocyte culture media and 50% BCEC culture media (outlined above).[40,41]

Hyperspectral imaging of PBCA-PS80-rhodamine NPs in astrocytes

Primary rat brain astrocytes were plated at a density of 50 000 cells/cover slip, incubated at 37 °C and 5% CO₂ for 48 h, and treated with 125 µg/ml PBCA-Rhodamine-PS80 NPs for 24 h. Cells were fixed in ice cold methanol for 10 min, and the coverslips were mounted on slides for hyperspectral analysis. The CytoViva Optical and Hyperspectral Imaging System (CytoViva, Auburn, AL) were used to capture and analyze the images. The scanned astrocytes were imaged at 100× with an Olympus BX-43 Microscope equipped with the patented CytoViva illumination system and a 100W quartz-halogen light source. Spectral data were captured with the CytoViva spectrophotometer and integrated CCD camera. Spectral analysis was performed with the CytoViva hyperspectral analysis software program.

Cytotoxicity bioassay

The metabolic activity of living cells was evaluated using the TOX-8 Resazurin-Based *In Vitro* Toxicology Assay Kit (Sigma-Aldrich) on media collected 24 h and 48 h after exposure to NPs, according to the manufacturer's instructions. Samples were then measured using a SpectraMax® 190 spectrophotometer (Molecular Devices, Sunnyvale, CA). Absorbance measurements were made at 600 nm with a reference wavelength of 690 nm that was subtracted from the primary wavelength measurement. The assays were performed three times, in quadruplicate, using primary cell lines obtained from different animals (three biological replicates). The means of the absorbance values for each sample were calculated, and comparisons between controls and PBCA NP treatment groups were analyzed using SPSS (IBM Corp., Chicago, IL).

Real time (RT)-PCR gene analysis

RNA was isolated from cellular co-cultures using the RNeasy Mini Kit according to the manufacturer's instructions and included DNase treatment (SABiosciences, Valencia, CA). For each sample, RNA was quantified using a ND-1000 Spectrophotometer (Thermo Fisher Scientific) and converted into cDNA (SABiosciences) on a PTC-100 thermocycler (MJ Research, Hercules, CA). Apoptosis-related gene expression was evaluated using a Rat Apoptosis RT² Profiler PCR Array (PARN-012A) (SABiosciences) in a 7300 Real Time PCR System (Applied Biosystems, Foster City, CA). The assays were performed three times per time point, using primary cell lines obtained from different animals (three biological replicates). Statistical analysis was conducted using RT² Profiler™ PCR Array Data Analysis (SABiosciences) and SPSS (IBM Corp., Chicago, IL). Significance is reported from a one-way ANOVA with Dunnett *post-hoc* analysis.

Results

Hyperspectral imaging of PBCA-PS80-rhodamine NPs in astrocytes

Uptake and intracellular availability of the PBCA-PS80-Rhodamine NPs in astrocytes were determined by analyzing images using the CytoViva Optical and Hyperspectral Imaging System. First, a high signal-to-noise spectral image was obtained of PBCA-PS80-Rhodamine NPs in solution on a glass slide. The image exhibited a spectral signature that showed a prominent peak near 570 nm and an abrupt drop at shorter wavelengths (Figure 1A), thus providing a unique signal for spectral mapping of PBCA-PS80-Rhodamine NPs in astrocytes. Figure 1(B) is a hyperspectral image of an astrocyte following incubation with PBCA-PS80-Rhodamine NPs at a concentration of 125 µg/ml. The presence of PBCA-PS80-Rhodamine NPs in the astrocyte was confirmed by comparing the spectral signatures in Figure 1(A) to those shown in Figure 1 (B and C) shows, in red, the pixels that spectrally confirm the presence of PBCA-PS80-Rhodamine NPs in the astrocyte. PBCA-PS80-Rhodamine NPs were not mapped in the control cell, as indicated by the absence of red pixels in the image (Figure 1D).

Cytotoxicity bioassay

Cytotoxicity of uncoated PBCA, PBCA-PS80 and PBCA-PS80-DOX NPs was evaluated in the co-culture system using a resazurin-based toxicology assay. Cytotoxicity of the NPs was indicated as a function of reduced cellular metabolic activity exhibited by a decrease in the bio-reduction of the resazurin dye in the mitochondria.

Figure 2 shows the combined results from three resazurin assays, derived from three independent experiments and performed as three biological replicates. Twenty-four hours after NP exposure, significant toxicity compared to the negative control (untreated cells) was shown only in co-cultures treated with the highest concentration (500 µg/ml) of uncoated PBCA NPs and PBCA-PS80 NPs (Figure 2A), while cells exposed to the PBCA-PS80-DOX NPs showed significant toxicity at concentrations of 125 µg/ml and higher (Figure 2A; $F_{19,220} = 39.65$, $p < 0.001$). Following 48 h of exposure, the co-cultures demonstrated variable toxicity to the uncoated PBCA, showing a significant difference compared to the negative control at concentrations of 7.81, 125 and 500 µg/ml. However, at both the 7.81 and 125 µg/ml concentrations, these co-cultures were also significantly different compared to the positive control. In contrast, cells treated with PBCA-PS80 NPs only showed toxicity at the highest concentration (500 µg/ml; Figure 2B). Cells exposed to PBCA-PS80-DOX NPs showed significant toxicity compared to the negative control at concentrations of 125 µg/ml and higher (Figure 2B; $F_{19,220} = 34.76$, $p < 0.001$), similar to the results at the 24 h time point.

Real time (RT)-PCR gene analysis

Following treatment of co-cultures with NPs, the mRNA expression levels of 84 apoptosis-related genes were analyzed by quantitative RT-PCR. For this purpose, the three treatment groups (uncoated PBCA, PBCA-PS80 and PBCA-PS80-DOX NPs) were compared to untreated cells at both 8 h and 24 h following NP exposure and evaluated for ΔC_t , $2^{-\Delta C_t}$, expression relative to control and fold regulation. Fold regulation is equal to the expression relative to control for values ≥ 1 and to the negative reciprocal of expression relative to control for values < 1 . Tables 1–4 show ΔC_t values and

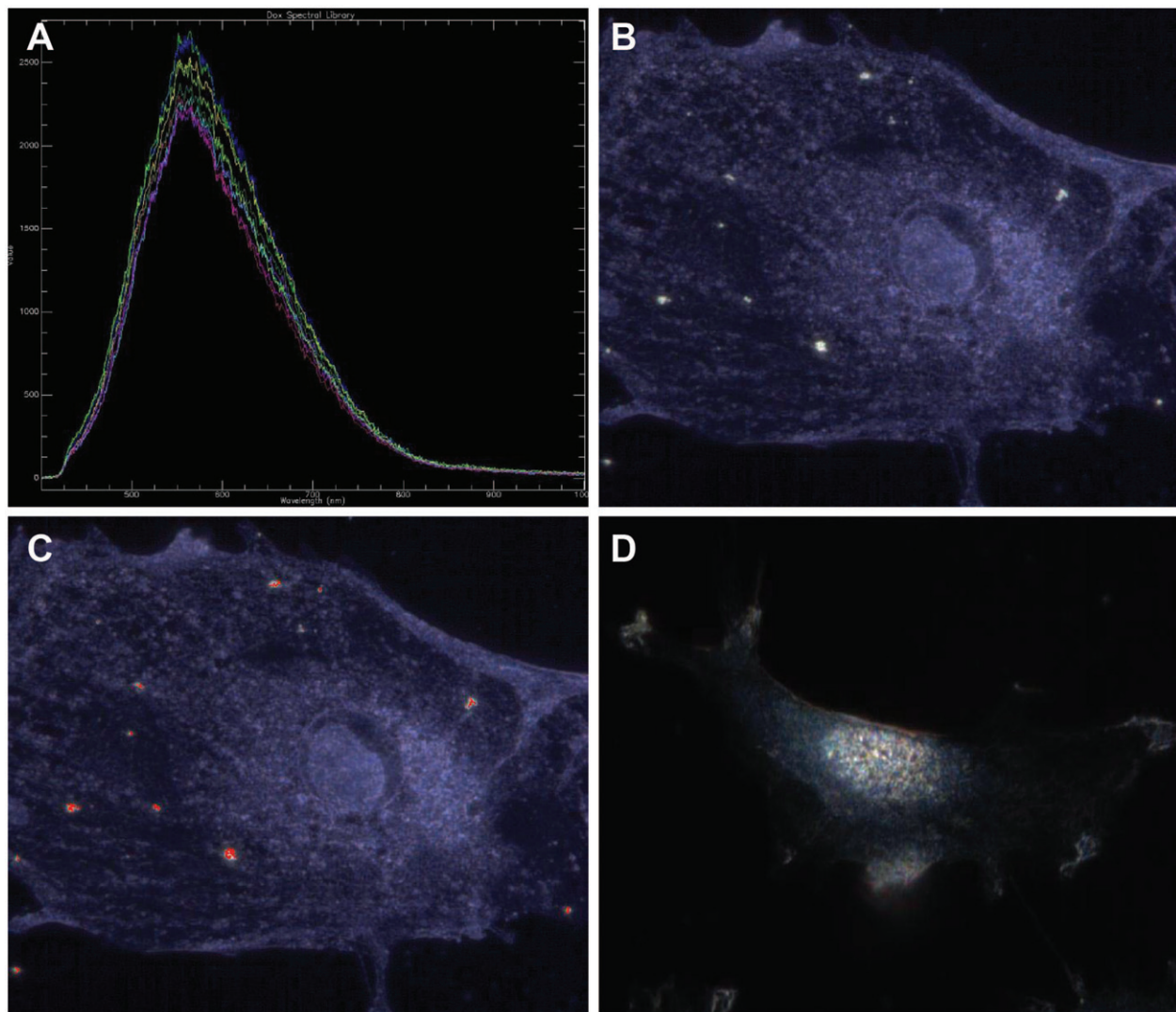


Figure 1. Hyperspectral imaging. (A) Spectral signature of PBCA-PS80-Rhodamine NPs in solution on a glass slide. (B) Hyperspectral image of an astrocyte following incubation with 125 µg/ml PBCA-PS80-Rhodamine NPs. (C) Same image as (B) showing in red the pixels that spectrally confirm the presence of PBCA-PS80-Rhodamine NPs in the astrocyte. (D) Hyperspectral image of an astrocyte not exposed to NP.

expressions relative to control for the 18 genes that showed significant changes in expression ($p < 0.05$), using a one-way ANOVA of $2^{-\Delta Ct}$ values. A complete list showing the alterations in these 18 genes for all experimental conditions is provided in Supplementary material (Supplemental Tables S1–S6). Co-cultures treated with PBCA-PS80-DOX NPs for 8 h showed significant mRNA downregulation of *Aven*, *Bcl10*, *Bnip1*, *Casp8*, *Casp9*, *Cflar*, *Cradd*, *Faim*, *Ripk2*, *Sphk2* and *Tradd* (at both 7.8 µg/ml and 31.25 µg/ml), *Apaf* and *Bcl2* (at 7.8 µg/ml) and *Bak1*, *Bcl2l1*, *Fadd* and *Traf2* (at 31.25 µg/ml) compared to untreated cells as determined by fold regulation analysis (Figures 3 and 4). *Cideb* was the only gene that exhibited significant upregulation at a concentration of 7.8 µg/ml (Figure 4A). *Tradd* is the only gene that showed altered expression when exposed to PBCA-PS80 and PBCA-PS80-DOX NPs for 24 h (Figure 3B).

These results indicate that co-cultures exposed to PBCA-PS80-DOX NPs exhibit alterations in apoptosis-related genes compared to untreated cells. The identified genes play roles in both the intrinsic, mitochondria-associated and extrinsic, receptor-associated, apoptotic pathways (Figure 5). No significant differences in the expression of apoptosis-related genes were detected in co-cultures exposed to uncoated PBCA NPs or PBCA-PS80 NPs at either time point (Figures 3 and 4).

Discussion

Poly(butylcyanoacrylate) (PBCA) NPs have great potential to serve as a vehicle for drug transport across the BBB, resulting in enhanced drug delivery to the brain,[21] but unintended cellular toxicity must be assessed. To accomplish this, an *in vitro* model of the BBB was used to evaluate cytotoxicity and apoptosis-related gene expression of co-cultured astrocytes and BCECs exposed to uncoated PBCA, PBCA-PS80 and PBCA-PS80-DOX NPs. This model of the BBB has been described previously and is shown to be consistent with *in vivo* BBB integrity. This was demonstrated by expression of P-glycoprotein in ECs, and the presence of efficient tight junctions, as demonstrated by positive staining for ZO-1 and occludin. In addition, functionality of the BBB model was confirmed by measuring the permeability coefficients of sucrose and insulin.[40,42–44]

Previous studies indicated no significant difference in toxicity between PS80-coated and uncoated PBCA NPs at concentrations up to 20 µg/ml.[18,22] Our results further support this idea in two ways: (i) co-cultures exposed to PBCA-PS80 NPs demonstrated low to no cytotoxicity, as determined by resazurin assays; (ii) PBCA-PS80 NP treated co-cultures did not show significant changes in apoptosis-related gene expression. Given the potential of PS80 to

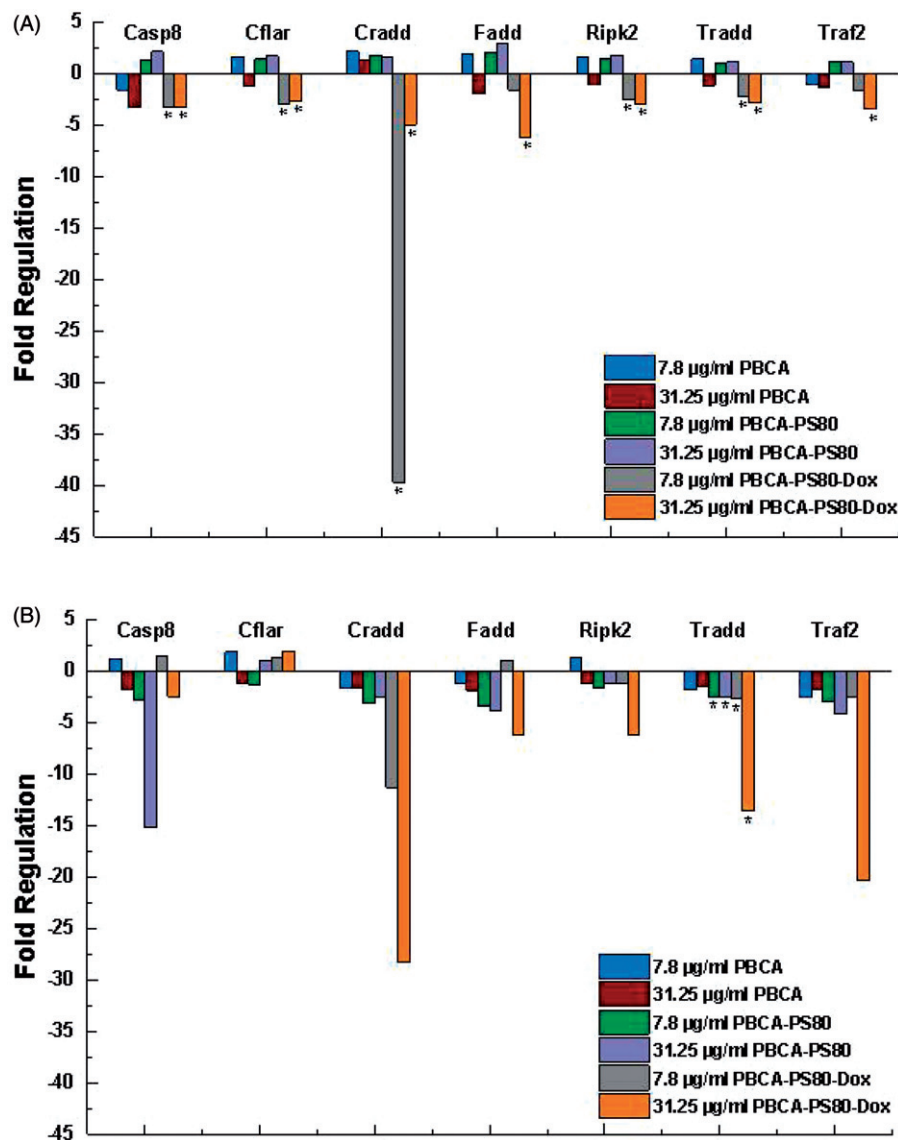


Figure 3. Changes in fold regulation of significant genes related to the Tnfr1 pathway. (A) Co-cultures exposed to varying NPs for 8 h; and (B) Co-cultures exposed to varying NPs for 24 h. Differences in expression that were found to be significant ($p < 0.05$) are marked with an asterisk.

uncoated PBCA or PBCA-PS80 NPs following both 24 h and 48 h exposure to the co-cultures (Figure 2).

Results from the cytotoxicity assays were further complemented by those obtained from RT-PCR. Co-cultures exposed to PBCA-PS80-DOX exhibited differential expression (particularly after 8 h of exposure) in genes related to both the *intrinsic*, mitochondria-associated and *extrinsic*, Tnfr1-associated apoptotic pathways currently known to play a role in DOX toxicity (Figures 3 and 4). DOX is known to induce pro-apoptotic activity of a key apoptotic transcription factor, Nf- κ b, in a non-canonical mechanism by provoking degradation of its inhibitory subunits (I κ k).[45]

Canonical Nf- κ b regulation is the *extrinsic* pathway and involves the binding of Tnf- α to Tnfr1 and subsequent recruitment of the signaling proteins Tradd, Traf2 and Rip. Traf2, Rip and I κ k then go on to activate Nf- κ b (Figure 5). This receptor-mediated activation is thought to lead to anti-apoptotic activity of Nf- κ b. Our data show downregulation of the genes encoding the Tradd, Traf2 and Rip proteins, which would prevent Nf- κ b from using this pathway for survival signaling (Figure 3A). However, it is important to note that this same signaling complex is able to recruit caspase 1 (Casp1) and continue the apoptotic caspase cascade.[46] In addition, the Tradd/

Traf2/Rip complex may signal apoptosis after internalization into the cytosol and dissociation from Tnfr1. Rip and Tradd then bind the Fas-inducing death domain (Fadd) adaptor molecule and ultimately recruit caspase 8 (Casp8).[47,48] Casp8 may then be inhibited by Cflar (Flip/Casper), directly continuing the *intrinsic*, receptor-associated apoptotic caspase cascade, or begin cross-talk with the *intrinsic* mitochondria-associated apoptotic mechanism (Figure 5). To facilitate this cross-talk, Casp8 would have to cleave Bid. Truncated Bid (tBid) can then translocate to the mitochondrion, leading to the oligomerization of Bak, ultimately resulting in the release of cytochrome C (CytoC). [47,49] For this reason, it was somewhat surprising that downregulation of the genes encoding Tradd, Traf2, Ripk2, Fadd and Cflar was observed when the co-culture was exposed to PBCA-PS80-DOX NPs for 8 h (Figure 3A).

Another Tnfr1-related, *extrinsic* signaling complex that can be recruited upon Tnf- α binding consists of Cradd (Raidd) and Rip. These proteins recruit caspase 2 (Casp2), which leads to the continuation of the receptor-associated apoptotic caspase cascade.[46] Interestingly, Cradd showed a large, significant downregulation when the co-culture was exposed to 7.81 µg/ml PBCA-PS80-DOX NPs for 8 h (Figure 3A).

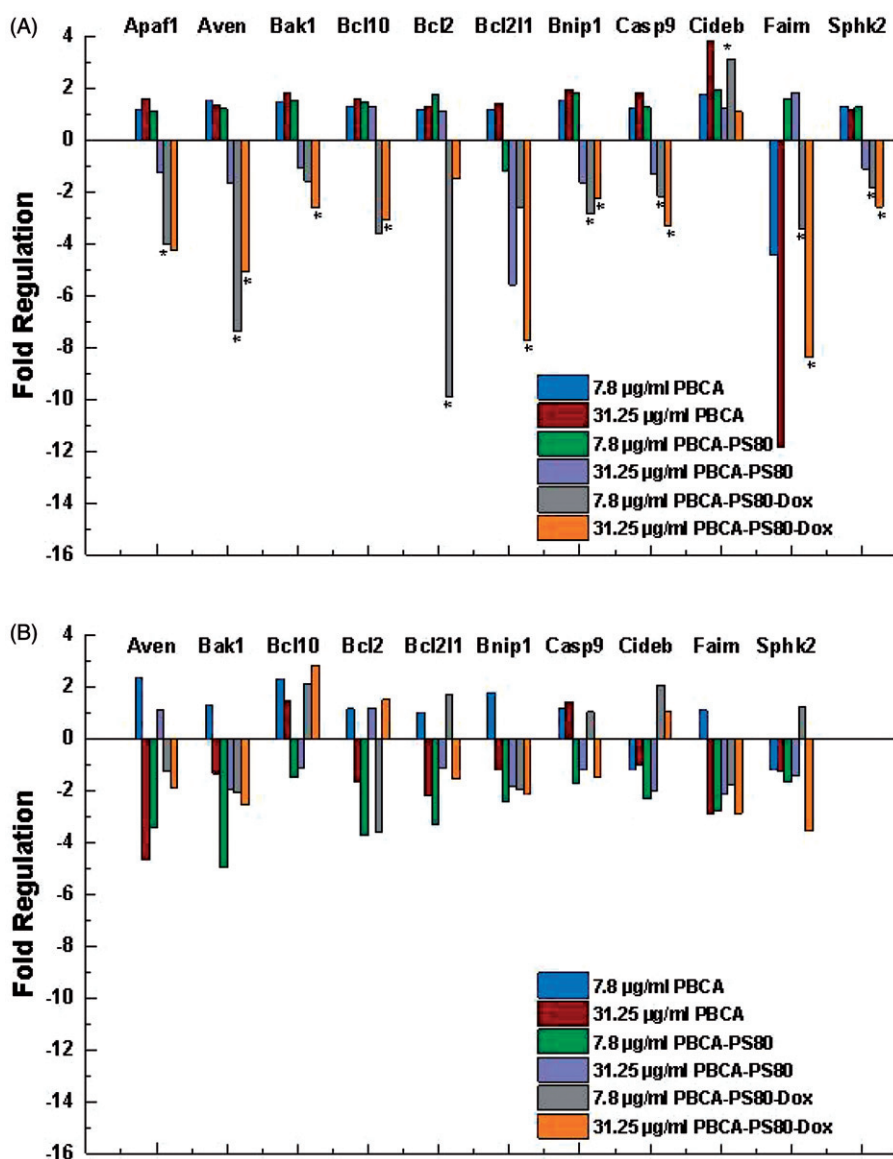


Figure 4. Changes in fold regulation of significant genes related to intrinsic apoptotic pathways. (A) Co-cultures exposed to varying NPs for 8 h; and (B) Co-cultures exposed to varying NPs for 24 h. Apaf1 exhibited an undetectable Ct response in one of the control replicates, so it is not represented here. Differences in expression that were found to be significant ($p < 0.05$) are marked with an asterisk.

As previously mentioned, the unintended toxicity of DOX often involves activation of the *intrinsic*, mitochondria-associated apoptotic pathway in response to ROS. This study showed significant downregulation of a few of the genes implicated in this pathway after 8 h of exposure to PBCA-PS80-DOX NPs: *Apaf1*, *Aven*, *Bak1*, *Bcl10*, *Bcl2*, *Bcl2l1*, *Bnip1*, *Casp8* and *Faim* (Figure 4A). The Bcl family of proteins is key to regulation of this pathway. Bcl2 is an anti-apoptotic protein found in the membrane of the mitochondrion and is opposed by the pro-apoptotic proteins Bax and Bak. Normal cells work to maintain a homeostatic ratio of Bcl2 to Bak to contain CytoC inside the mitochondrion. Should Bax or Bak be present in levels to overpower Bcl2, CytoC would be released from the mitochondrion and into the cytosol.[24,49] Cytosolic CytoC is capable of joining with Apaf1 to activate caspase 9 (Casp9) through the formation of an apoptosome. Activation of the apoptosome causes subsequent caspase cleavage, ultimately resulting in apoptosis. The anti-apoptotic protein, Aven, works to prevent this pathway upstream by activating Bcl2l1 (Bclxl) (an inhibitor of the Bax/Bak proteins) and downstream by inhibiting Apaf1.[50,51] Faim, another anti-apoptotic protein, was recently indicated to

function downstream of Bax and Casp9 to inhibit subsequent caspase activity. It is also interesting to note that Sole and colleagues demonstrated that overexpression of Faim promoted the nuclear localization of Nf- κ b.[52] The pro-apoptotic protein Bnip1 has recently been found to regulate mitochondrial fission depending on levels of dynamin-related protein 1 (Drp1) and Bcl2.[53] Another *intrinsic*, mitochondria-associated, pro-apoptotic protein, Cideb,[54] was observed to be significantly upregulated when the co-culture was exposed to 7.81 μg/ml PBCA-PS80-DOX NPs for 8 h.

Modulations in the expression of many of these genes were expected to be observed due to the ability of DOX to increase endogenous levels ROS and Tnf- α . However, it was surprising that an overwhelming majority of the genes, both pro- and anti-apoptotic, were downregulated. Regarding this downregulation, it is important to note that the timing of biochemical events in apoptosis depends on several factors, including time, cell type, inducing agent, drug concentration and/or stimulus intensity. It is likely that activation of these genes is an early event following exposure of the co-cultures to PBCA-PS80-DOX NPs, so that by the 8 h time

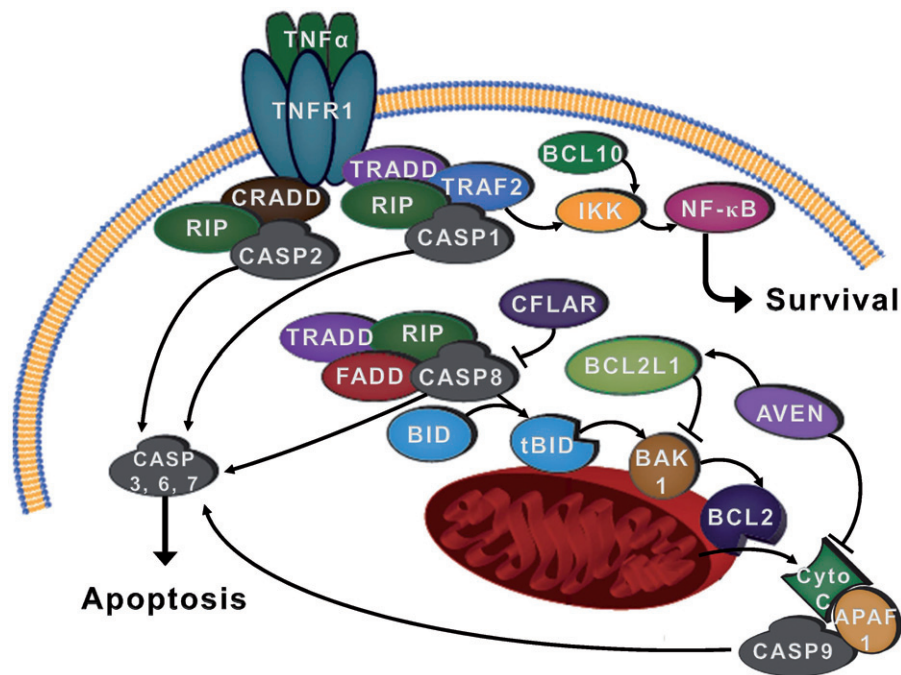


Figure 5. This characterization of the Tnf-superfamily signaling pathway and its cross-talk with the mitochondria-associated, intrinsic apoptotic pathway outlines protein interactions leading to either cell death or survival. Tnf-alpha is an inflammatory cytokine that binds to its associated receptor, causing death domain complexes to recruit proteins needed to ensure cell survival or death through apoptosis. Casp8 recruitment to the internalized Tradd/Rip/Fadd signaling complex and subsequent activation is able to truncate Bid, thus allowing its translocation to the mitochondria. This cross-talk from the Tnfr1 pathway may lead to cell death through mitochondrial-mediated apoptosome formation and subsequent caspase activation. The intrinsic mitochondrial-mediated apoptosis pathway is able to be activated by a number of different signaling proteins, including p53.

point, these genes are being down-regulated. This may be further supported by the lack of significance in all gene expression (except the downregulation of Tradd) after 24 h of treatment. It is also likely that the astrocytes and endothelial cells are undergoing different apoptotic mechanisms, as was described by Punsawad et al. in their study of cerebral malaria.[55] Specifically, Nf-kb was greatly responsible for modulating apoptosis in brain endothelial cells, but was not largely implicated in glial apoptosis.[55] A variety of different factors are known to be responsible for controlling astrocyte apoptosis, and the pathway is often dependent on the cause of cellular stress.[56]

Conclusion

In conclusion, significant cytotoxicity was not observed when the co-culture model was exposed to PBCA NPs and PBCA-PS80 NPs except for the highest, most unlikely, therapeutic concentrations. Modulations in receptor-associated and mitochondria-associated pathways have been well characterized in unintended DOX toxicity.[24,25,28,57,58] Many of the same apoptotic proteins showed altered gene expression in our analysis. This suggests that the cellular response to DOX may be the same for both delivery methods (free DOX or DOX loaded PBCA-PS80 NPs) and indicates that PBCA-PS80 NPs are an effective vehicle for delivery of DOX and other potential treatments for CNS conditions.

Acknowledgements

The authors would like to thank Dr. Stephen Linn (Department of Biological Sciences, NKU) and Dr. Celeste Morris (Department of Chemistry, NKU) for their contributions to this work. In addition, the authors would like to acknowledge the late Dr. Heather Bullen for her conceptualization and contributions to this work.

Disclosure statement

This research was supported by the National Institutes of Health (NINDS) 1R15NS067548-01A1, Kentucky NSF EPSCoR, Merck/AAAS Undergraduate Science Research Program, National Center for Research Resources Grant P20 RR16481 (Fellowship), NKU Research Foundation and NKU CINSAM (to K. L. H).

References

1. Pardridge WM. Brain drug targeting: the future of brain drug development. Cambridge (NY): Cambridge University Press; 2001. xvii, 353 p., 4 plates p.
2. Fernandes C, Soni U, Patravale V. Nano-interventions for neurodegenerative disorders. *Pharmacol Res* 2010;62:166–78.
3. Omidi Y, Barar J. Impacts of blood-brain barrier in drug delivery and targeting of brain tumors. *Bioimpacts* 2012;2:5–22.
4. Wolburg H, Lippoldt A. Tight junctions of the blood-brain barrier: development, composition and regulation. *Vascul Pharmacol* 2002;38:323–37.
5. Pardridge WM. Alzheimer's disease drug development and the problem of the blood-brain barrier. *Alzheimers Dement* 2009;5:427–32.
6. Gilmore JL, Yi X, Quan L, Kabanov AV. Novel nanomaterials for clinical neuroscience. *J Neuroimmune Pharmacol* 2008;3: 83–94.
7. Kolter M, Ott M, Hauer C, et al. Nanotoxicity of poly(n-butylcyanoacrylate) nanoparticles at the blood-brain barrier, in human whole blood and in vivo. *J Control Release* 2015;197:165–79.
8. Reimold I, Domke D, Bender J, et al. Delivery of nanoparticles to the brain detected by fluorescence microscopy. *Eur J Pharm Biopharm* 2008;70:627–32.

9. Kreuter J, Alyautdin RN, Kharkevich DA, Ivanov AA. Passage of peptides through the blood-brain barrier with colloidal polymer particles (nanoparticles). *Brain Res* 1995;674:171–4.
10. Kurakhmaeva KB, Djindjikhshvili IA, Petrov VE, et al. Brain targeting of nerve growth factor using poly(butyl cyanoacrylate) nanoparticles. *J Drug Target* 2009;17:564–74.
11. Yang H. Nanoparticle-mediated brain-specific drug delivery, imaging, and diagnosis. *Pharm Res* 2010;27:1759–71.
12. Schneider T, Becker A, Ringe K, et al. Brain tumor therapy by combined vaccination and antisense oligonucleotide delivery with nanoparticles. *J Neuroimmunol* 2008;195:21–7.
13. Darius J, Meyer FP, Sabel BA, Schroeder U. Influence of nanoparticles on the brain-to-serum distribution and the metabolism of valproic acid in mice. *J Pharm Pharmacol* 2000;52:1043–7.
14. Schroeder U, Schroeder H, Sabel BA. Body distribution of ³H-labelled dalargin bound to poly(butyl cyanoacrylate) nanoparticles after i.v. injections to mice. *Life Sci* 2000;66:495–502.
15. Schroeder U, Sommerfeld P, Sabel BA. Efficacy of oral dalargin-loaded nanoparticle delivery across the blood-brain barrier. *Peptides* 1998;19:777–80.
16. Schroeder U, Sabel BA. Nanoparticles, a drug carrier system to pass the blood-brain barrier, permit central analgesic effects of i.v. dalargin injections. *Brain Res* 1996;710:121–4.
17. Sommerfeld P, Sabel BA, Schroeder U. Long-term stability of PBCA nanoparticle suspensions. *J Microencapsul* 2000;17:69–79.
18. Kreuter J. Nanoparticulate systems for brain delivery of drugs. *Adv Drug Deliv Rev* 2001;47:65–81.
19. Steiniger SC, Kreuter J, Khalansky AS, et al. Chemotherapy of glioblastoma in rats using doxorubicin-loaded nanoparticles. *Int J Cancer* 2004;109:759–67.
20. Gulyaev AE, Gelperina SE, Skidan IN, et al. Significant transport of doxorubicin into the brain with polysorbate 80-coated nanoparticles. *Pharm Res* 1999;16:1564–9.
21. Schroeder U, Sabel BA, Schroeder H. Diffusion enhancement of drugs by loaded nanoparticles in vitro. *Prog Neuropsychopharmacol Biol Psychiatry* 1999;23:941–9.
22. Wang CX, Huang LS, Hou LB, et al. Antitumor effects of polysorbate-80 coated gemcitabine polybutylcyanoacrylate nanoparticles in vitro and its pharmacodynamics in vivo on C6 glioma cells of a brain tumor model. *Brain Res* 2009;1261:91–9.
23. Kreuter J, Gelperina S. Use of nanoparticles for cerebral cancer. *Tumori* 2008;94:271–7.
24. Tacar O, Sriamornsak P, Dass CR. Doxorubicin: an update on anticancer molecular action, toxicity and novel drug delivery systems. *J Pharm Pharmacol* 2013;65:157–70.
25. Wang S, Konorev EA, Kotamraju S, et al. Doxorubicin induces apoptosis in normal and tumor cells via distinctly different mechanisms intermediacy of H(2)O(2)- and p53-dependent pathways. *J Biol Chem* 2004;279:25535–43.
26. Minotti G, Menna P, Salvatorelli E, et al. Anthracyclines: molecular advances and pharmacologic developments in antitumor activity and cardiotoxicity. *Pharmacol Rev* 2004;56:185–229.
27. Gewirtz DA. A critical evaluation of the mechanisms of action proposed for the antitumor effects of the anthracycline antibiotics adriamycin and daunorubicin. *Biochem Pharmacol* 1999;57:727–41.
28. Carvalho C, Santos RX, Cardoso S, et al. Doxorubicin: the good, the bad and the ugly effect. *Curr Med Chem* 2009;16:3267–85.
29. Kotamraju S, Konorev EA, Joseph J, Kalyanaraman B. Doxorubicin-induced apoptosis in endothelial cells and cardiomyocytes is ameliorated by nitron spin traps and ebselen. Role of reactive oxygen and nitrogen species. *J Biol Chem* 2000;275:33585–92.
30. Tacar O, Dass CR. Doxorubicin-induced death in tumour cells and cardiomyocytes: is autophagy the key to improving future clinical outcomes? *J Pharm Pharmacol* 2013;65:1577–89.
31. Riad A, Bien S, Gratz M, et al. Toll-like receptor-4 deficiency attenuates doxorubicin-induced cardiomyopathy in mice. *Eur J Heart Fail* 2008;10:233–43.
32. Usta Y, Ismailoglu UB, Bakkaloglu A, et al. Effects of pentoxifylline in adriamycin-induced renal disease in rats. *Pediatr Nephrol* 2004;19:840–3.
33. Olivier JC. Drug transport to brain with targeted nanoparticles. *NeuroRx* 2005;2:108–19.
34. Gratton SE, Ropp PA, Pohlhaus PD, et al. The effect of particle design on cellular internalization pathways. *Proc Natl Acad Sci USA* 2008;105:11613–18.
35. Farokhzad OC, Langer R. Impact of nanotechnology on drug delivery. *ACS Nano* 2009;3:16–20.
36. Voigt N, Henrich-Noack P, Kockentiedt S, et al. Surfactants, not size or zeta-potential influence blood-brain barrier passage of polymeric nanoparticles. *Eur J Pharm Biopharm* 2014;87:19–29.
37. Gelperina S, Maksimenko O, Khalansky A, et al. Drug delivery to the brain using surfactant-coated poly(lactide-co-glycolide) nanoparticles: influence of the formulation parameters. *Eur J Pharm Biopharm* 2010;74:157–63.
38. Powers KW, Palazuelos M, Moudgil BM, Roberts SM. Characterization of the size, shape, and state of dispersion of nanoparticles for toxicological studies. *Nanotoxicology* 2007;1:42–51.
39. Weiss C, Kohnle M, Landfester K, et al. The first step into the brain: uptake of NIO-PBCA nanoparticles by endothelial cells in vitro and in vivo, and direct evidence for their blood-brain barrier permeation. *ChemMedChem* 2008;3:1395–403.
40. Garcia-Garcia E, Gil S, Andrieux K, et al. A relevant in vitro rat model for the evaluation of blood-brain barrier translocation of nanoparticles. *Cell Mol Life Sci* 2005;62:1400–8.
41. Szabo CA, Deli MA, Ngo TK, Joo F. Production of pure primary rat cerebral endothelial cell culture: a comparison of different methods. *Neurobiology (Bp)* 1997;5:1–16.
42. Garcia CM, Darland DC, Massingham LJ, D'Amore PA. Endothelial cell-astrocyte interactions and TGF beta are required for induction of blood-neural barrier properties. *Brain Res Dev Brain Res* 2004;152:25–38.
43. de Boer AG, Gaillard PJ. In vitro models of the blood-brain barrier: when to use which? *Curr Med Chem Central Nerv Syst Agents* 2002;2:203–9.
44. Garberg P, Ball M, Borg N, et al. In vitro models for the blood-brain barrier. *Toxicol In Vitro* 2005;19:299–334.
45. Ashikawa K, Shishodia S, Fokt I, et al. Evidence that activation of nuclear factor-kappaB is essential for the cytotoxic effects of doxorubicin and its analogues. *Biochem Pharmacol* 2004;67:353–64.
46. Mathew SJ, Haubert D, Kronke M, Leptin M. Looking beyond death: a morphogenetic role for the TNF signalling pathway. *J Cell Sci* 2009;122:1939–46.

47. Eum HA, Vallabhaneni R, Wang Y, et al. Characterization of DISC formation and TNFR1 translocation to mitochondria in TNF- α -treated hepatocytes. *Am J Pathol* 2011;179:1221–9.
48. Schneider-Brachert W, Tchikov V, Neumeyer J, et al. Compartmentalization of TNF receptor 1 signaling: internalized TNF receptors as death signaling vesicles. *Immunity* 2004;21:415–28.
49. Wei MC, Lindsten T, Mootha VK, et al. tBID, a membrane-targeted death ligand, oligomerizes BAK to release cytochrome c. *Genes Dev* 2000;14:2060–71.
50. Kutuk O, Temel SG, Tolunay S, Basaga H. Aven blocks DNA damage-induced apoptosis by stabilising Bcl-xL. *Eur J Cancer* 2010;46:2494–505.
51. Melzer IM, Fernandez SB, Bossier S, et al. The Apaf-1-binding protein Aven is cleaved by Cathepsin D to unleash its anti-apoptotic potential. *Cell Death Differ* 2012;19:1435–45.
52. Sole C, Dolcet X, Segura MF, et al. The death receptor antagonist FAIM promotes neurite outgrowth by a mechanism that depends on ERK and NF-kappa B signaling. *J Cell Biol* 2004;167:479–92.
53. Ryu SW, Choi K, Yoon J, et al. Endoplasmic reticulum-specific BH3-only protein BNIP1 induces mitochondrial fragmentation in a Bcl-2- and Drp1-dependent manner. *J Cell Physiol* 2012;227:3027–35.
54. Chen Z, Guo K, Toh SY, et al. Mitochondria localization and dimerization are required for CIDE-B to induce apoptosis. *J Biol Chem* 2000;275:22619–22.
55. Punsawad C, Maneerat Y, Chaisri U, et al. Nuclear factor kappa B modulates apoptosis in the brain endothelial cells and intravascular leukocytes of fatal cerebral malaria. *Malar J* 2013;12:260.
56. Takuma K, Baba A, Matsuda T. Astrocyte apoptosis: implications for neuroprotection. *Prog Neurobiol* 2004;72:111–27.
57. Chiosi E, Spina A, Sorrentino A, et al. Change in TNF-alpha receptor expression is a relevant event in doxorubicin-induced H9c2 cardiomyocyte cell death. *J Interferon Cytokine Res* 2007;27:589–97.
58. Gopinath S, Vanamala SK, Gujrati M, et al. Doxorubicin-mediated apoptosis in glioma cells requires NFAT3. *Cell Mol Life Sci* 2009;66:3967–78.